The importance of pickup oxygen ion precipitation to the Mars upper atmosphere under extreme solar wind conditions

Xiaohua Fang,[1] Stephen W. Bougher,[2] Robert E. Johnson,[3] Janet G. Luhmann,[4] Yingjuan Ma,[5] Yung-Ching Wang,[4] and Michael W. Liemohn[2]

Received 6 March 2013; revised 22 March 2013; accepted 25 March 2013; published 30 May 2013.

[1] While the Mars upper atmosphere is continuously bombarded by charged particles of solar and planetary origins, the energy flux carried is often not sufficient to significantly affect the neutral atmosphere. However, we show that this is not the case during major space weather events. By applying two Mars global models—a Monte Carlo model for simulating pickup O^+ precipitation at the exobase and a thermosphere-ionosphere model for assessing its global impact, we find that the thermospheric effects of reentering ions can change from negligible to very important when upstream solar wind conditions vary from normal to extreme. The atmospheric response under the most extreme conditions includes dramatic neutral temperature enhancement, significant neutral composition and wind changes, and increased importance of sputtering loss and possibly even thermal escape of heavy species. **Citation:** Fang, X., S. W. Bougher, R. E. Johnson, J. G. Luhmann, Y. Ma, Y.-C. Wang, and M. W. Liemohn (2013), The importance of pickup oxygen ion precipitation to the Mars upper atmosphere under extreme solar wind conditions, *Geophys. Res. Lett.*, *40*, 1922–1927, doi:10.1002/grl.50415.

1. Introduction

[2] There are two main sources of energetic ions that continuously and impulsively hit the Mars upper atmosphere: protons from the solar wind and from solar energetic particle events, and planetary ions that originate in the neutral atmosphere and are subsequently picked up and accelerated by the fields in the solar wind. Ion precipitation and their impact on the Mars atmosphere has been extensively studied: e.g., *Brecht* [1997], *Kallio and Janhunen* [2001], *Leblanc et al.* [2002], and *Ulusen et al.* [2012] for H^+; *Luhmann and Kozyra* [1991], *Johnson et al.* [2000], *Leblanc and Johnson* [2002], *Chaufray et al.* [2007], and *Li et al.* [2011] for O^+.

[3] These studies are either 1-D models of aeronomical effects (i.e., local heating/ionization rates) or focused on escape (i.e., sputtering and production of the neutral corona). Under typical solar wind conditions, the absorbed energy in the upper atmosphere from precipitating H^+/O^+ ions is no more than a few percent of the solar EUV energy and thus has a negligible effect on the thermal properties [*Kallio and Janhunen*, 2001], but might affect atmospheric loss by momentum transfer collisions [*Luhmann and Kozyra*, 1991]. However, the importance of impacting ions under extreme space weather conditions is poorly understood. Here we focus on pickup O^+ precipitation and report the first attempt to evaluate the atmospheric response under disturbed solar wind conditions from a global perspective.

2. Method

[4] The challenges to model pickup ion impact on the upper atmosphere are 3-fold: first, to globally trace pickup ion trajectories near Mars and to obtain detailed spatial and velocity distributions for reentering ions; second, to calculate local energy deposition; and third, to assess the global atmospheric response.

[5] For the first aspect, the Monte Carlo Pickup Ion Transport model (MCPIT) developed by *Fang et al*. [2008, 2010a, 2010b] is employed to derive energy spectra and angular distributions of precipitating particles, within the electromagnetic field environment described by a 3-D multispecies MHD model [*Ma et al.*, 2004; *Ma and Nagy*, 2007]. The photo-ionization frequency in the MHD calculations in this study is appropriate for solar maximum conditions. *Ma and Nagy* [2007] performed global MHD solar wind interaction simulations for a range of solar and interplanetary conditions in order to assess the impact of enhanced interplanetary conditions on the ion escape. In the calculations described here, a large number of test particles (over 4 billion) are released within the MCPIT simulation domain, extending from 300 km altitude up to 5 Martian radii away from the planet center. By properly monitoring and weighting each reentering test particle, we obtain detailed distributions of the impacting O^+ flux at the exobase altitude on a 5° × 5° longitude-by-latitude grid. The precipitation is calculated with an energy resolution of $\Delta E/E = \sim 20\%$ and an angular resolution of 5°.

[6] We apply 1-D range calculation for incident O^+ ions within each energy and angular bin, and then integrate over them to obtain the concomitant local energy deposition. Since the ions rapidly neutralize through charge exchange collisions, based on the Monte Carlo simulations in *Johnson et al.* [2000], the maximum atmospheric column mass (in amu/cm^2) that an incident oxygen atom can penetrate is $M \approx 1.8 \times 10^{16}\,(8E+2)\cos(\alpha)$, where α is the incident angle and E is the energy in keV. That such an approximation is applicable can be understood from *Johnson*

[1]Laboratory for Atmospheric and Space Physics, University of Colorado, Boulder, Colorado, USA.
[2]Department of Atmospheric, Oceanic and Space Sciences, University of Michigan, Ann Arbor, Michigan, USA.
[3]Engineering Physics, University of Virginia, Charlottesville, Virginia, USA.
[4]Space Sciences Laboratory, University of California, Berkeley, California, USA.
[5]Institute of Geophysics and Planetary Physics, University of California, Los Angeles, California, USA.

Corresponding author: X. Fang, Laboratory for Atmospheric and Space Physics, University of Colorado, 3665 Discovery Drive, Boulder, CO 80303, USA. (xiaohua.fang@lasp.colorado.edu)

©2013. American Geophysical Union. All Rights Reserved.
0094-8276/13/10.1002/grl.50415

Table 1. Upstream Solar Wind Conditions Used for the Perturbation Cases

Perturbation Cases	Solar Wind Density (cm^{-3})	Solar Wind Speed (km/s)	Interplanetary Magnetic Field (nT)
quiet	4	400	3 (Parker spiral, 56°)
active	4	1200	3 (B_y only)
extreme	20	1000	20 (B_y only)

[1994], where it is seen that, at low energies, the average penetration varies nearly linearly with E until at very low energies incident atoms rattle around and lose their energy in a narrow layer of gas at about the exobase altitude. Along the penetration depth, the input energy is lost mostly to neutral heating [*Luhmann and Kozyra*, 1991]. The heating rate (in units of keV/cm^3/s) is $q(z) \approx \rho(z)\phi_E/M$, where ρ is the atmospheric mass density in amu/cm^3 and ϕ_E is the incident energy flux in keV/cm^2/s. This estimate of the O^+ induced heating is then incorporated into the 3-D Mars Thermospheric General Circulation Model (MTGCM) [e.g., *Bougher et al.*, 2006, 2009] to investigate the global effects. The MTGCM solves densities for the major neutral species (CO_2, CO, N_2, and O) and several photochemically produced ions (O_2^+, CO_2^+, O^+, and NO^+ below 200 km altitude) as well as neutral winds. In this study, O^+ heating is calculated at each MTGCM time step, assuming that the pickup ion precipitation patterns are held fixed both in space (with respect to local time) and over the time period of the integration (about 10 Martian days).

[7] In order to test the importance of precipitating pickup O^+ to the upper atmosphere, we carried out calculations for one baseline case and three perturbation cases. The baseline simulation is a regular MTGCM case with particle impact neglected and under the conditions appropriate for nominal solar maximum ($F_{10.7}$ = 200 at Equinox). The perturbation cases are identical to the baseline case with the same solar EUV input, except that the heating by precipitating pickup O^+ under different solar wind plasma conditions (summarized in Table 1) is added into the MTGCM. We use the terms "quiet", "active", and "extreme" to describe the three activity levels of impinging solar wind conditions. The MHD field and plasma solutions for the quiet and extreme cases have been discussed by *Ma et al.* [2004] and *Ma and Nagy* [2007], respectively. While extreme events are not a regular phenomenon, they occur several times per solar cycle in the current epoch. For example, an extremely intense coronal mass ejection (much stronger than what we examined in this paper) was recently observed at 1 AU on 23 July 2012, having a speed of >1500 km/s and a magnetic field strength of > 80 nT [e.g., *Dryer et al.*, 2012].

[8] We chose the upstream convection electric fields to have the same direction (i.e., toward the north), so that the MSO (Mars-Solar-Orbital) and MSE (Mars-Sun-Electric field) coordinate systems overlap. Moreover, the strongest crustal fields face the Sun with a subsolar longitude of 180°W in all cases, excluding complications arising from the crustal fields at different local times as demonstrated by *Fang et al.* [2010b] and *Li et al.* [2011]. Although our model results apply to this specific geometrical arrangement of Sun, Martian crustal fields, and interplanetary field, the results are expected to represent general trends.

3. Model Results

[9] Figure 1 shows the MCPIT model calculated energy flux distributions of reentering pickup O^+ at 300 km altitude for the three perturbation cases. As the external plasma

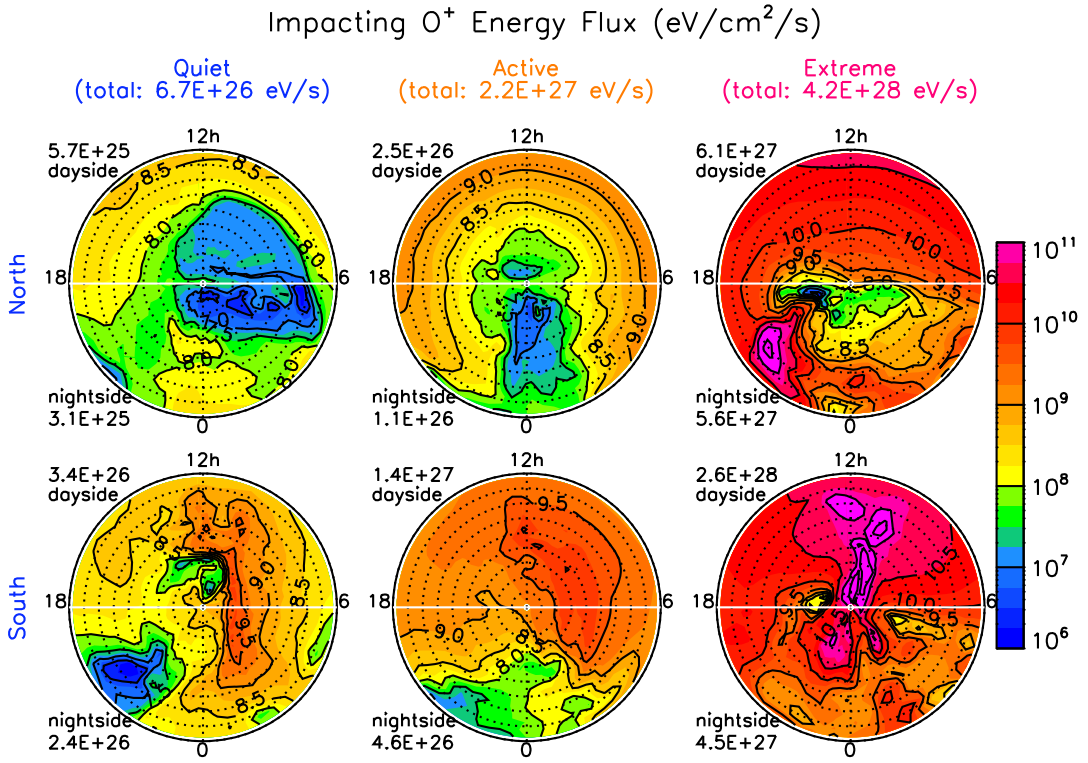

Figure 1. Reentering O^+ energy flux distributions in the (top) northern and (bottom) southern hemispheres. The columns from left to right give the results in the quiet, active, and extreme cases, respectively.

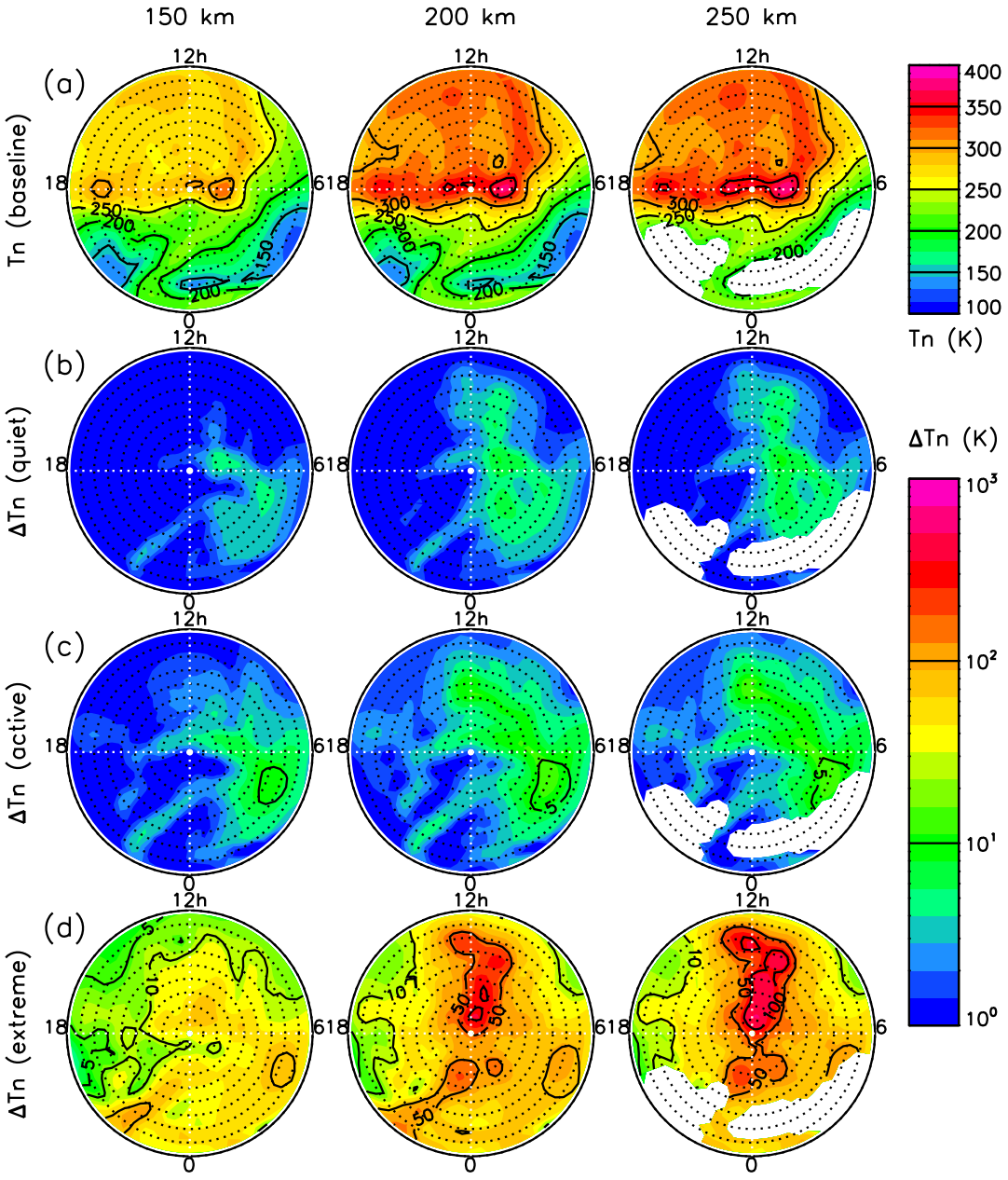

Figure 2. (a) Neutral temperature in the southern hemisphere in the baseline case, and (b to d) temperature changes between the three perturbation cases and the baseline case. The contour curves in Figures 2c and 2d show the regions at the percentage difference levels of 5%, 10%, 50%, and 100%. The three columns (from left to right) show the results at 150, 200, and 250 km altitudes, respectively.

conditions become severe, the incident flux is considerably intensified over the whole energy range in general. When the solar wind changes from quiet to active, the total energy input to the upper atmosphere increases from 6.7×10^{26} to 2.2×10^{27} eV/s, by a factor of 3. In the extreme case, the value is remarkably enhanced by nearly two orders of magnitude to 4.2×10^{28} eV/s, having a dayside-averaged intensity of 0.06 mW/m^2. On the other hand, by scaling the current solar EUV energy flux at Earth (5.1 mW/m^2) to the Mars orbit and considering a heating efficiency of ~0.2 in the Mars atmosphere [*Bougher et al.*, 2009], we estimate an effective solar EUV energy flux (for heating) of 0.4 mW/m^2 at Mars, which is more than seven times larger than the averaged O^+ energy flux even in the extreme case.

[10] However, a note of caution is needed when making this comparison. First, unlike solar radiation, precipitating particles are distributed highly nonuniformly. It is demonstrated in Figure 1 that reentering O^+ energy fluxes vary considerably over relatively short spatial ranges. The intensity can be up to as high as 2.4 mW/m^2 in the extreme case, which clearly dominates solar EUV heating. Moreover, O^+ precipitation exhibits a strong hemispheric asymmetry: ~70%–90% of energy being deposited in the southern hemisphere for this geometry. Second, there is a distinct difference on the altitude where the energy of incident photon, H^+, and O^+ is absorbed in the Mars atmosphere. According to *Kallio and Janhunen* [2001], *Leblanc et al.* [2002], and *Sheel et al.* [2012], H^+ energy deposition peaks at

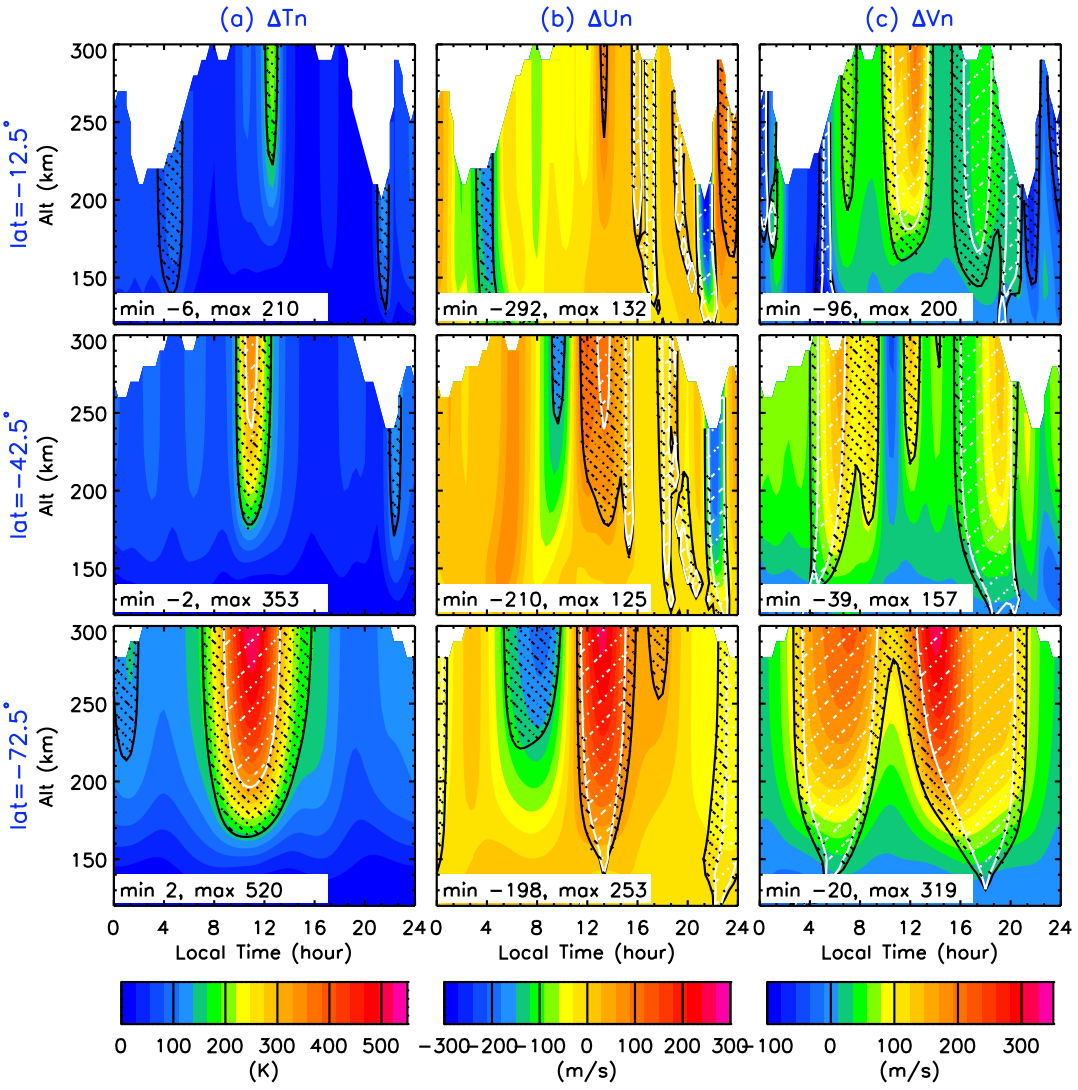

Figure 3. Thermospheric responses to the extreme event in terms of the changes in (a) neutral temperature, (b) zonal wind, and (c) meridional wind. The zonal wind is defined as positive for the eastward direction and the meridional wind is positive for northward. The results are shown at three latitudes: (top) –12.5°, (middle) –42.5°, and (bottom) –72.5°. The black and white curves mark the absolute percentage difference levels of 50% and 100%, respectively. The black and white shadings represent a considerable change by 50–100% and >100%, respectively.

~120 km altitude or lower. This overlaps with the altitude region from solar EUV/UV, making precipitating H^+ less efficient in its competition with solar radiation. In contrast, as illustrated by *Luhmann and Kozyra* [1991] and confirmed by our calculations for the quiet case, precipitating O^+ loses most of its energy above ~140 km altitude. Therefore, the separation of the energy deposition zone of precipitating O^+ from solar EUV and precipitating H^+ provides O^+ a competitive advantage in affecting the Mars upper atmosphere. Actually, in accordance with the upper atmospheric lift due to O^+ energy input in our extreme case (shown later), the globally averaged peak heating altitude is elevated to around 175 km. As the particle induced heating is calculated from a mass density column at every time step, the modification of the upper atmosphere is self-consistently considered in the MTGCM simulations. Note that in this study we neglect the feedback of atmospheric changes to the pickup process, which may happen in two ways. First, the enhanced upper atmosphere and corona increase pickup ion production; Second, the altered atmosphere changes solar wind mass loading and thus the electromagnetic field distributions that influences precipitating pickup ion fluxes and spectra. These feedback mechanisms, as well as the impact on the competition between atmospheric heating and cooling (due to thermal conduction, horizontal winds, and escape), need to be addressed with multiple iterations among the MTGCM, MHD, and MCPIT model calculations.

[11] Our results are in line with previous studies. The hemispherically averaged energy spectrum in our quiet case (solar max) is in remarkably close agreement with *Luhmann et al.* [1992] and *Chaufray et al.* [2007] high solar activity results, both in shape and in intensity (not shown here due to space limit). For instance, our globally averaged number flux and energy flux in the quiet case are 7.3×10^6 /cm^2/s and 3.9×10^8 eV/cm^2/s, respectively, while the corresponding values by *Chaufray et al.* [2007] are

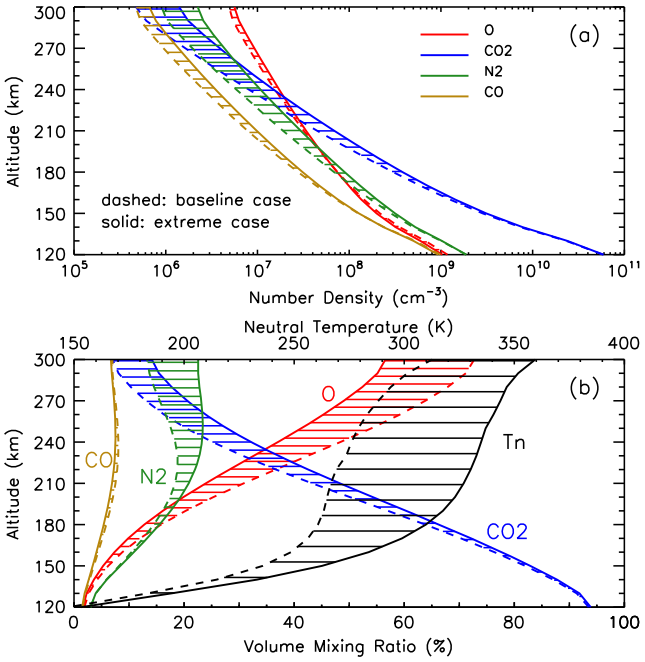

Figure 4. The variation in the globally averaged (a) number densities and (b) mixing ratios and temperature for neutral species between the baseline and extreme cases. The temperature profiles (black) are given with the scale on the top axis.

3.0×10^6 and 2.6×10^8. The factor of ~2 or less difference is partly attributed to different model treatments and resolutions. It should be emphasized that precipitating particles have a complex distribution, not only depending on spatial locations, as already seen in Figure 1, but also non-Maxwellian in energy and anisotropic in angle. Numerical experiments in which we assumed an isotropic Maxwellian flux for the active case doubled the temperature increase. Therefore, the globally-averaged distributions used in previous studies mask considerable regional variability as well as the 2-D spectrum in energy and angle space. In this study, we take advantage of the MCPIT capability of tracing each particle's motion, and calculate detailed spectral information for precipitating particles everywhere at the exobase.

[12] Figure 2 shows the comparison of the southern thermospheric neutral temperature in the absence or presence of pickup O^+ precipitation in the MTGCM. The white areas correspond to the regions above the topmost pressure level of the model. It is seen that the response in temperature when the solar wind condition is normal (quiet case) is noticeable but not significant. The maximum enhancement is 9 K, or about 3% in terms of percentage. In the active case, the temperature increases by up to 15 K (7%), which is important enough to be tested by future Mars orbiters. More importantly, the calculations show that when the extremely disturbed solar wind impinges on Mars, the input energy carried by precipitating pickup ions is so large (at least regionally) that the temperature responds dramatically in the upper atmosphere. The temperature rises by more than 10% throughout almost the whole southern thermosphere above 150 km. In particular, the maximum increase at 250 km altitude is 520 K (155%) on the dayside and 223 K (96%) on the nightside. These increases occur in the places with large particle energy inputs as illustrated in Figure 1.

[13] Figure 3 provides another look at the thermospheric response under extreme conditions. Besides the temperature increase (except for few sparse areas), the changes in zonal and meridional winds are shown as a function of local time and altitude. It is seen that when the solar wind is extreme, the bombardment of precipitating O^+ ions can produce major changes in temperature and in neutral winds, not only in magnitude but also in significance. There are large regions (mainly above 150 km altitude) having changes ≥50% in absolute value. Unlike the important temperature enhancement mostly focusing on the dayside in accordance with the ion energy input, the effect on the thermal transport by wind exhibits a more complex pattern. Because advection in the upper atmosphere is significantly affected, the 1-D aeronomical models that were employed to capture vertical variations are no longer appropriate, rather, a global description as demonstrated in the MTGCM is needed.

[14] Figure 4 reveals the globally averaged composition changes induced by the O^+ precipitation. The compositions for the quiet and active periods are very close to those in the baseline case and not shown here for clarity. The increase in the upper atmospheric heating rate under the extreme conditions and its nonuniformity drive the upper atmospheric expansion and composition changes as seen by comparing the extreme to baseline cases. CO_2 and N_2 number densities are enhanced above 120 km altitude, whereas O (CO) densities are slightly depleted below around 185 (145) km and then increase at higher altitude regions. Their volume mixing ratios, on the other hand, demonstrate a simpler pattern of change. Throughout the upper atmosphere above 120 km, the mixing ratios of CO_2 (N_2) are enhanced by up to 8% (9%) in the extreme case, while the O (CO) mixing ratios drop by up to 16% (1%). The globally averaged temperature is raised by up to 61 K from the baseline to the extreme case. The actual range of the changes can be much bigger or smaller locally than the globally averaged values (see Figures 2 and 3). In addition to composition changes due to enhanced diffusion and transport, the incident particle radiation can cause mixing and chemistry. Therefore, more detailed studies are required, with special attention to the changes in temperature-gradient-induced atmospheric dynamics, diffusion and mixing, and chemistry.

4. Discussion and Conclusion

[15] In addition to the pickup process, the Mars atmosphere can also be sputtered by reentering energetic particles [*Luhmann and Kozyra*, 1991]. The sputtering loss for the cases considered here has recently been reported by *Wang et al.* [2012] using a coupled Monte Carlo and molecular dynamic calculation approach of *Leblanc and Johnson* [2002], as given in Table 2. As a comparison, we calculated a sputtering to pickup loss ratio of 0.27 for the quiet case, in agreement with the value of 0.23 by *Chaufray et al.* [2007].

Table 2. Particle Precipitation and Escape

Perturbation Cases	Pickup O^+ Escape (s^{-1})	Reentering O^+ (s^{-1})	Sputtered O Escape (s^{-1})	Ratio[a]
quiet	4.1×10^{24}	1.3×10^{25}	1.1×10^{24}	0.27
active	1.6×10^{25}	3.3×10^{25}	2.2×10^{24}	0.18
extreme	4.8×10^{25}	9.2×10^{25}	5.4×10^{25}	1.13

[a] Ratio of sputtering loss to pickup loss.

More interestingly, it is found that although sputtering may not be competitive in atmospheric loss when the solar wind is quiet, its importance is largely elevated and underscored by a high ratio of 1.13 when the solar wind is extremely disturbed. This is because of the increase in the mean energy of precipitating particles.

[16] The high rates of energy deposition in the exobase region by O^+ precipitation will enhance the importance of escape. In 1-D models, a rough upper bound for thermal escape plus sputtering is given by the energy-limited rate, the energy deposited per unit time in the upper atmosphere divided by the escape energy ($\sim$2 eV for Mars). In the extreme case, this would imply an upper limit of approximately $2c\times10^{28}$ oxygen per second, where c is oxygen fraction at the exobase. This would be a huge effect. However, based on the results in Figure 3, care must be taken in applying 1-D models since it is seen that thermal transport by horizontal winds may be important. However, the transport by flow is somewhat overestimated in the MTGCM because the cooling due to escape is not included. A model which iteratively includes both aspects is being developed.

[17] Understanding atmospheric impact from precipitating ions under disturbed solar winds is important for two reasons. First, the net atmospheric loss over billions of years is an important consideration for planetary evolution studies and is not correctly estimated by averaging over the variable flux over time. Since the ancient atmosphere of Mars was subject to more frequent extreme space weather events, this can have a profound effect on the estimate of the net atmospheric loss. Second, understanding the atmospheric changes during extreme space weather events on Mars today is critical to planning robotic and human exploration of Mars.

[18] This study clearly illustrates that, although pickup ion precipitation into the Mars upper atmosphere under normal conditions can be omitted, it must be considered when a major space weather event takes place. Under extreme conditions, particle heating is so important as to regionally overwhelm solar EUV heating, significantly alter atmospheric advection and composition, and enhance atmospheric loss. There are a few improvements needed. By assuming hydrostatic equilibrium and ignoring cooling by escape, the MTGCM could overestimate advection and underestimate the effect of vertical transport. In addition, as in *Chaufray et al.* [2007], feedback between the expanded upper atmosphere and the neutral corona can influence the pickup ion precipitation process. Such additions are in progress.

[19] **Acknowledgments.** The work was supported by NSF grants AST-0908472 and AST-0908311, and NASA grants NNX11AN38G, NNX10AO17G, and NNX12AG57G. The Editor thanks Paul Withers and an anonymous reviewer for their assistance in evaluating this paper.

References

Bougher, S. W., J. R. Murphy, J. M. Bell, M. A. Lopez-Valverde, and P. G. Withers (2006), Polar warming in the Mars lower thermosphere: Seasonal variations owing to changing insolation and dust distributions, *Geophys. Res. Lett.*, *33*, L02203, doi:10.1029/2005GL024059.

Bougher, S. W., T. M. McDunn, K. A. Zoldak, and J. M. Forbes (2009), Solar cycle variability of Mars dayside exospheric temperatures: Model evaluation of underlying thermal balances, *Geophys. Res. Lett.*, *36*, L05201, doi:10.1029/2008GL036376.

Brecht, S. H. (1997), Hybrid simulations of the magnetic topology of Mars, *J. Geophys. Res.*, *102*(A3), 4743–4750, doi:10.1029/96JA03205.

Chaufray, J. Y., R. Modolo, F. Leblanc, G. Chanteur, R. E. Johnson, and J. G. Luhmann (2007), Mars solar wind interaction: Formation of the martian corona and atmospheric loss to space, *J. Geophys. Res.*, *112*, E09009, doi:10.1029/2007JE002915.

Dryer, M., K. Liou, C. Wu, S. Wu, N. Rich, S. Plunkett, L. Simpson, C. Fry, and K. Schenk (2012), Extreme fast coronal mass ejection on 23 July 2012*, Abstract SH44B-04 Presented at 2012 Fall Meeting*, AGU, San Francisco, Calif., 3-7 Dec.

Fang, X., M. W. Liemohn, A. F. Nagy, Y. Ma, D. L. De Zeeuw, J. U. Kozyra, and T. H. Zurbuchen (2008), Pickup oxygen ion velocity space and spatial distribution around Mars, *J. Geophys. Res.*, *113*, A02210, doi: 10.1029/2007JA012736.

Fang, X., M. W. Liemohn, A. F. Nagy, J. Luhmann, and Y. Ma (2010a), On the effect of the martian crustal magnetic field on atmospheric erosion, *Icarus*, *206*, 130–138, doi:10.1016/j.icarus.2009.01.012.

Fang, X., M. W. Liemohn, A. F. Nagy, J. G. Luhmann, and Y. Ma (2010b), Escape probability of martian atmospheric ions: Controlling effects of the electromagnetic fields, *J. Geophys. Res.*, *115*, A04308, doi: 10.1029/2009JA014929.

Johnson, R. E. (1994), Plasma-induced sputtering of an atmosphere, *Space Sci. Rev.*, *69*, 215–253.

Johnson, R. E., D. Schnellenberger, and M. C. Wong (2000), The sputtering of an oxygen thermosphere by energetic O+, *J. Geophys. Res.*, *105*, 1659.

Kallio, E., and P. Janhunen (2001), Atmospheric effects of proton precipitation in the Martian atmosphere and its connection to the Mars-solar wind interaction, *J. Geophys. Res.*, *106*, 5617, doi:10.1029/2000JA000239.

Leblanc, F., and R. E. Johnson (2002), Role of molecular species in pickup ion sputtering of the martian atmosphere, *J. Geophys. Res.*, *107*(E2), 5010, doi:10.1029/2000JE001473.

Leblanc, F., J. G. Luhmann, R. E. Johnson, and E. Chassefiere (2002), Some expected impacts of a solar energetic particle event at Mars, *J. Geophys. Res.*, *107*(A5), 1058, doi:10.1029/2001JA900178.

Li, L., Y. Zhang, Y. Feng, X. Fang, and Y. Ma (2011), Oxygen ion precipitation in the martian atmosphere and its relation with the crustal magnetic fields, *J. Geophys. Res.*, *116*, A08204, doi:10.1029/2010JA016249.

Luhmann, J. G., and J. U. Kozyra (1991), Dayside pickup oxygen ion precipitation at Venus and Mars: Spatial distributions, energy deposition and consequences, *Geophys. Res. Lett.*, *19*(2), 2151–2154.

Luhmann, J. G., R. E. Johnson, and M. Zhang (1992), Evolutionary impact of sputtering of the martian atmosphere by O^+ pickup ions, *J. Geophys. Res.*, *96*(A4), 5457, doi:10.1029/90JA01753.

Ma, Y., A. F. Nagy, I. V. Sokolov, and K. C. Hansen (2004), Three-dimensional, multispecies, high spatial resolution MHD studies of the solar wind interaction with Mars, *J. Geophys. Res.*, *109*, A07211, doi: 10.1029/2003JA010367.

Ma, Y.-J., and A. F. Nagy (2007), Ion escape fluxes from Mars, *Geophys. Res. Lett.*, *34*, L08201, doi:10.1029/2006GL029208.

Sheel, V., S. A. Haider, P. Withers, K. Kozarev, I. Jun, S. Kang, G. Gronoff, and C. Simon Wedlund (2012), Numerical simulation of the effects of a solar energetic particle event on the ionosphere of Mars, *J. Geophys. Res.*, *117*, A05312, doi:10.1029/2011JA017455.

Ulusen, D., D. A. Brain, J. G. Luhmann, and D. L. Mitchell (2012), Investigation of Mars' ionospheric response to solar energetic particle events, *J. Geophys. Res.*, *117*, A12306, doi:10.1029/2012JA017671.

Wang, Y.-C., J. G. Luhmann, F. Leblanc, X. Fang, R. E. Johnson, Y. Ma, W.-H. Ip, and L. Li (2012), Modeling of the sputtering efficiency for Martian atmosphere*, Abstract P23A-1907 presented at 2012 fall meeting*, AGU, San Francisco, Calif., 3-7 Dec.